

$\mathcal{O}(N_f\alpha^2)$ Corrections to Muon Decay

Robin G. Stuart

*Randall Laboratory of Physics
Ann Arbor, Michigan 48109-1120, USA*

Abstract

The calculation of the $\mathcal{O}(N_f\alpha^2)$ corrections to muon decay is described. These are the 2-loop diagrams containing a massless fermion loop and they form an important gauge-invariant subclass. It is shown that all such diagrams can be expressed in terms of a universal master integral. We focus on the calculation of box diagrams and in particular on the removal of their infrared divergences.

1 Introduction

Muon decay, $\mu^- \rightarrow \nu_\mu e^- \bar{\nu}_e$, has always been a proving ground for both pure QED and electroweak radiative corrections [1–3]. Until recently the muon decay coupling constant, G_μ , and the electromagnetic coupling constant, α , were by far the best measured electroweak observables and played a pivotal rôle as input to the Standard Model. The accuracy of theoretical predictions was limited by the errors on M_Z which was taken as the third input required to make the model predictive. Now the situation has changed somewhat. Both M_Z and G_μ are determined to an accuracy of 2×10^{-5} and it may be possible to reduce the error on M_Z still further if the LEP beam energy calibration can be better understood.

By comparison electroweak calculations have attained an precision of only a few permill. Obviously it would be desirable to have the results of full 2-loop electroweak calculations at our disposal and considerable progress has been made in this direction [4]. Such calculations are likely to be intractable when expressed in analytic form and in practice one would quote only numerical results. There do exist, however, a few 2-loop calculations for which exact analytic results

can be obtained in a compact closed form [3, 5–8]. Here we discuss one such set of corrections. These are dubbed $\mathcal{O}(N_f\alpha^2)$ corrections to muon decay, where N_f is the number of light fermions. Because N_f is quite large, the $\mathcal{O}(N_f\alpha^2)$ corrections are expected to be a dominant subset of 2-loop graphs and since N_f provides a unique tag, the complete set of $\mathcal{O}(N_f\alpha^2)$ corrections contributing to a particular physical process will form a gauge-invariant set. Diagrams of this type have been considered in connection with the muon anomalous magnetic moment [9].

A priori the $\mathcal{O}(N_f\alpha^2)$ corrections can be expected to contribute at the level of 1.5×10^{-4} . Without their calculation and inclusion, theoretical predictions remain uncertain at least at this level.

If the fermions are assumed to be massless compared to M_W , an excellent approximation for all but the third generation, then the only ‘dimensionful’ quantities appearing in the calculation are M_W , M_Z and M_H and there are very few diagrams containing a Higgs. The contributions from diagrams not involving Higgs bosons can then only be a polynomial in $\sin^2\theta_W$ with coefficients involving $\ln \cos^2\theta_W$, $\ln \pi$ and Euler’s constant, γ .

Assuming massless fermions reduces the topologies of diagrams that must be considered since the fermions can then only couple to vector bosons but not to Goldstones. However, the calculation is still a fully-fledged 2-loop electroweak calculation requiring the complete renormalization of the Standard Model at $\mathcal{O}(N_f\alpha^2)$. Although muon decay represents a zero momentum transfer process, much can be learned from it about the cancellation of divergences in high-energy processes. Indeed unlike the case of the calculation of $\mathcal{O}(\alpha^2 m_t^4)$ corrections to the ρ -parameter [5, 6, 8], there is a proliferation of diagrams involving counterterms and these constitute significant fraction of the effort involved.

In addition to the calculation of diagrams at zero momentum transfer one also requires the W and Z^0 mass counterterms that must be obtained by evaluating diagrams at high scales. In principle this can be done in any renormalization scheme using methods expounded in ref.s [10, 11] but the work is considerably reduced by adopting the $\overline{\text{MS}}$ scheme in which only the simpler divergent parts of the diagrams are

required.

In this talk we will summarize some of the salient features of the calculation. In section 2 the master integral will be given and in section 3 we will concentrate on contributions coming from box diagrams. Diagrams of this type do not occur in other 2-loop electroweak calculations performed to date. It will be shown how the IR divergences can be separated from these diagrams in a well-defined manner that permits them to be meshed with bremsstrahlung diagrams.

The work reported here was undertaken with R. Akhoury and P. Malde. Full details of the general methods used can be found in ref. [12] and results for muon decay in ref. [13].

2 The Master Integral

In what follows an anticommuting γ_5 is assumed. A Euclidean metric with the square of time-like momenta being negative will be used and all calculations will be done in $R_{\xi=1}$ gauge. The sine and cosine of the weak mixing angle, θ_W , will be denoted s_θ and c_θ respectively. γ_L and γ_R are the usual left- and right-handed helicity projection operators.

Many, but by no means all, $\mathcal{O}(N_f\alpha^2)$ diagrams are obtained simply by inserting a fermion loop into the boson propagator of a one-loop diagram. Because the original one-loop diagram is often logarithmically divergent, the fermion loop insertion will need to be calculated to $\mathcal{O}(n-4)$ in dimensional regularization, where n is the dimension of space-time. It turns out, however, that for all $\mathcal{O}(N_f\alpha^2)$ diagrams occurring in low-energy processes, it is possible to obtain expressions that are exact in n .

For the massless fermion loop insertion, it may be shown that

$$\begin{array}{c} \text{~~~~~} \bullet \text{~~~~~} \\ \text{~~~~~} \circ \text{~~~~~} \\ \text{~~~~~} \bullet \text{~~~~~} \\ \text{~~~~~} \end{array} = - \left(\delta_{\mu\nu} - \frac{p_\mu p_\nu}{p^2} \right) (\beta_L \beta'_L + \beta_R \beta'_R) \frac{(n-2)}{(n-1)} \int \frac{d^n q}{i\pi^2} \frac{p^2}{q^2 (q+p)^2} \quad (1)$$

where β_L , β_R and β'_L , β'_R of the couplings of the attached vector bosons.

For processes at zero momentum transfer it is possible to immediately reduce all tensor integrals that occur to scalar integrals by using projection operator techniques [12]. These scalar integrals can then be written as expressions involving a general master integral,

$$\begin{aligned} & \int \frac{d^n p}{i\pi^2} \frac{1}{[p^2]^j [p^2 + M^2]^k} \int \frac{d^n q}{i\pi^2} \frac{1}{[q^2]^l [(q+p)^2]^m} \\ &= \frac{\pi^{n-4}}{(M^2)^{k+j+l+m-n}} \Gamma\left(l+m-\frac{n}{2}\right) \Gamma\left(\frac{n}{2}-l\right) \Gamma\left(\frac{n}{2}-m\right) \\ & \times \frac{\Gamma(n-j-l-m) \Gamma(k+j+l+m-n)}{\Gamma\left(\frac{n}{2}\right) \Gamma(k) \Gamma(l) \Gamma(m) \Gamma(n-l-m)} \end{aligned} \quad (2)$$

3 Box Diagrams

A useful set of identities for calculating one-loop box diagrams appears in ref. [14]. They are, however, valid only for $n = 4$ because of their intended use at one-loop. For general n it may be shown that these relations become

$$\begin{aligned} [\gamma_\rho \gamma_\mu \gamma_\sigma \gamma_{L,R}]_1 [\gamma_\rho \gamma_\nu \gamma_\sigma \gamma_{L,R}]_2 &= 4\delta_{\mu\nu} [\gamma_\alpha \gamma_{L,R}]_1 [\gamma_\alpha \gamma_{L,R}]_2 \\ &+ (n-4) [\gamma_\mu \gamma_{L,R}]_1 [\gamma_\nu \gamma_{L,R}]_2 \end{aligned} \quad (3)$$

$$\begin{aligned} [\gamma_\rho \gamma_\mu \gamma_\sigma \gamma_{L,R}]_1 [\gamma_\rho \gamma_\nu \gamma_\sigma \gamma_{R,L}]_2 &= 4 [\gamma_\nu \gamma_{L,R}]_1 [\gamma_\mu \gamma_{R,L}]_2 \\ &+ (n-4) [\gamma_\mu \gamma_{L,R}]_1 [\gamma_\nu \gamma_{R,L}]_2 \end{aligned} \quad (4)$$

$$\begin{aligned} [\gamma_\rho \gamma_\mu \gamma_\sigma \gamma_{L,R}]_1 [\gamma_\sigma \gamma_\nu \gamma_\rho \gamma_{L,R}]_2 &= 4 [\gamma_\nu \gamma_{L,R}]_1 [\gamma_\mu \gamma_{L,R}]_2 \\ &+ (n-4) [\gamma_\mu \gamma_{L,R}]_1 [\gamma_\nu \gamma_{L,R}]_2 \end{aligned} \quad (5)$$

$$\begin{aligned} [\gamma_\rho \gamma_\mu \gamma_\sigma \gamma_{L,R}]_1 [\gamma_\sigma \gamma_\nu \gamma_\rho \gamma_{R,L}]_2 &= 4\delta_{\mu\nu} [\gamma_\alpha \gamma_{L,R}]_1 [\gamma_\alpha \gamma_{R,L}]_2 \\ &+ (n-4) [\gamma_\mu \gamma_{L,R}]_1 [\gamma_\nu \gamma_{R,L}]_2 \end{aligned} \quad (6)$$

where the square brackets $[]_1$ and $[]_2$ indicate that the enclosed γ -matrices are associated with the separate external fermion currents J_1 and J_2 respectively. These identities, along with projection operator techniques, may be used to reduce box diagrams to the form $I \cdot \mathcal{M}_0$ where I is a scalar integral and \mathcal{M}_0 is the Born level matrix element.

All $\mathcal{O}(N_f \alpha^2)$ box diagrams correspond to the insertion of a fermion loop into boson propagators in one-loop box diagrams. The box dia-

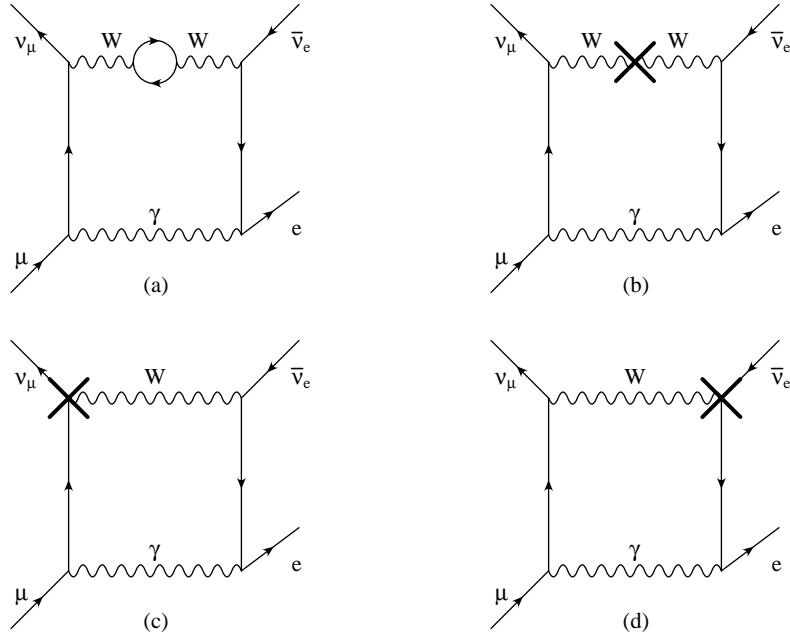


Figure 1: A class of box diagrams containing UV and IR divergences.

grams, so obtained, are either logarithmically divergent or have double poles at $n = 4$ corresponding to mixed UV and IR divergences or fermion mass singularities.

Consider the diagrams of Fig.1. The crosses represent fermionic parts of $\mathcal{O}(\alpha)$ counterterms. The fermion loop contribution in Fig.1a vanishes at $q^2 = 0$ where q is the 4-momentum in the photon propagator and the diagram is thus IR finite. If the counterterms on the W line in Fig.1b–d together vanish at $q^2 = 0$ then they too will be IR finite however this depends on the renormalization scheme that is chosen and is not generally the case. It happens, for example, in the $\overline{\text{MS}}$ but not in the on-shell renormalization scheme.

In Fig.1b–d the insertion of counterterms corresponds to replacing

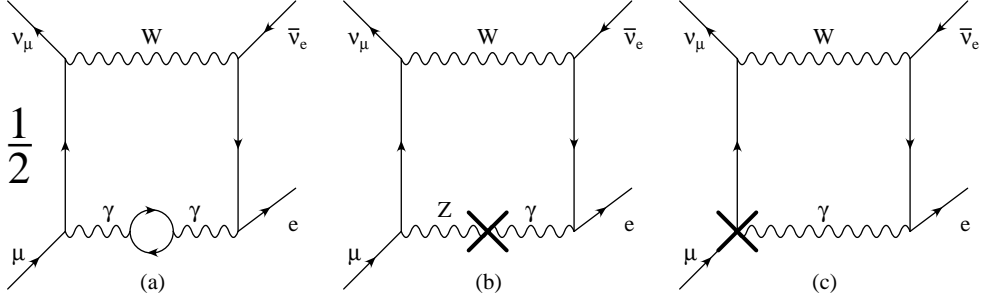


Figure 2: A class of box diagrams containing UV and IR divergences and fermion mass singularities.

the W propagator in the one-loop box diagram

$$\frac{1}{q^2 + M_W^2} \rightarrow \left(2\frac{\delta g}{g}\right) \frac{1}{q^2 + M_W^2} - \frac{\delta M_W^2}{(q^2 + M_W^2)^2} \quad (7)$$

$$= \left(2\frac{\delta g}{g}\right) \frac{q^2}{(q^2 + M_W^2)^2} - \frac{M_W^2}{(q^2 + M_W^2)^2} \left\{ \left(2\frac{\delta g}{g}\right) - \frac{\delta M_W^2}{M_W^2} \right\} \quad (8)$$

where δg and δM_W^2 are the $SU(2)$ coupling constant counterterm and W mass counterterm respectively.

The first term of (8) yields an IR finite contribution and its UV divergences cancel against those of Fig.1a. The second term in (8) is UV finite but generates an IR divergence and must be combined with soft bremsstrahlung correction to produce a finite result. As mentioned above the last term vanishes in the $\overline{\text{MS}}$ scheme.

A similar thing happens for the diagrams shown in Fig.2 except that now Fig.2a is both IR divergent and has a fermion mass singularity. If we denote the fermion loop insertion in the photon propagator as $(q^2 \delta_{\mu\nu} - q_\mu q_\nu) \Pi'_{\gamma\gamma}(q^2)$ then we may write

$$\Pi'_{\gamma\gamma}(q^2) = [\widehat{\Pi}'_{\gamma\gamma}(0)] + [\Pi'_{\gamma\gamma}(0) - \widehat{\Pi}'_{\gamma\gamma}(0)] + [\Pi'_{\gamma\gamma}(q^2) - \Pi'_{\gamma\gamma}(0)] \quad (9)$$

where

$$\widehat{\Pi}'_{\gamma\gamma}(0) = s_\theta^2 \frac{\delta g}{g} + c_\theta^2 \frac{\delta g'}{g'} \quad (10)$$

and g' is the $U(1)$ coupling constant.

The first term on the rhs of (9) yields an IR divergent correction that cancels against the IR divergences of the counterterm diagrams Fig.2b and 2c leaving an overall UV divergence. This remaining UV divergence cancels against those of other box diagrams involving Z^0 bosons. The second term in square brackets yields an IR divergent term that needs to be combined with soft bremsstrahlung diagrams to yield a finite result. Finally the third term gives a finite contribution that is singular for vanishing fermion masses. It will be subject to a hadronic contribution and should therefore be evaluated using dispersion relations. We do not consider the second and third term further.

Once IR divergences are removed in this way, the $\mathcal{O}(N_f\alpha^2)$ corrections to the Born level matrix element, \mathcal{M}_0 , coming from box diagrams may be written as $\mathcal{M}_0\Delta r^{(2)}$ where

$$\Delta r^{(2)} = \left(\frac{g^2}{16\pi^2} \right)^2 \left\{ \frac{2 \ln^2 c_\theta^2}{9s_\theta^4} (8s_\theta^8 + 12s_\theta^6 - 131s_\theta^4 + 135s_\theta^2 - 45) \right. \\ \left. - \frac{4}{3} \ln c_\theta^2 (2s_\theta^2 - 1) - s_\theta^2 [\Pi'_{\gamma\gamma}(-M_Z^2) - \Pi'_{\gamma\gamma}(0)] \right. \\ \left. + \frac{\ln c_\theta^2}{s_\theta^2} [\Pi'_{\gamma\gamma}(-M_Z^2) - \Pi'_{\gamma\gamma}(0)] (2s_\theta^4 - 10s_\theta^2 + 5) \right\} \quad (11)$$

for each massless fermion generation.

This result is given in the on-shell renormalization scheme and the photon vacuum polarization, $\Pi'_{\gamma\gamma}(-M_Z^2) - \Pi'_{\gamma\gamma}(0)$, arises from the definition of one-loop counterterms in this scheme. The corresponding expression in the $\overline{\text{MS}}$ scheme is somewhat longer because of the presence of terms such as $\ln M_W^2/\mu^2$ and $\ln \pi$.

References

- [1] T. Kinoshita and A. Sirlin, *Phys. Rev.* **113** (1959) 1652.
- [2] A. Sirlin, *Phys. Rev.* **D 22** (1980) 971.
- [3] A. Sirlin, *Phys. Rev.* **D 29** (1984) 89.
- [4] J. Franzkowski, these proceedings
- [5] J. J. van der Bij and F. Hoogeveen, *Nucl. Phys.* **B 283** (1987) 477.
- [6] R. Barbieri *et al.*, *Nucl. Phys.* **B 409** (1993) 105.
- [7] A. Denner, W. Hollik and B. Lampe, *Z. Phys.* **C 60** (1993) 193.
- [8] J. Fleischer, O. V. Tarasov and F. Jegerlehner, *Phys. Rev.* **D 51** (1995) 3820.
- [9] A. Czarnecki, B. Krause and W. Marciano, *Phys. Rev.* **D 52** (1995) 2619; A. Czarnecki, these proceedings
- [10] G. Weiglein, R. Scharf and M. Böhm, *Nucl. Phys.* **B 416** (1994) 606.
- [11] R. Scharf and J. B. Tausk, *Nucl. Phys.* **B 412** (1994) 523.
- [12] R. Akhoury, P. Malde and R. G. Stuart, preprint UM-TH-96-16.
- [13] R. Akhoury, P. Malde and R. G. Stuart, in preparation.
- [14] A. Sirlin, *Nucl. Phys.* **B 192** (1981) 93.